

Evaluation and Extension of the Flutter-Margin Method for Flight Flutter Prediction

S. J. Price*

McGill University, Montreal, Quebec, Canada

and

B. H. K. Lee†

Institute for Aerospace Research, Ottawa, Ontario, Canada

For a binary flutter the so-called flutter-margin method is a good way of extrapolating from subcritical flight test data to estimate the flutter speed; the best estimates are obtained with a linear extrapolation. Good estimates of the flutter speed can be obtained from data at speeds as low as 50% of the flutter speed. The flutter-margin is shown to be relatively insensitive to errors in the damping measurements, but is very sensitive to errors in frequency measurements. It does not give good predictions of the flutter speed when the instability is dominated by a single degree-of-freedom mechanism. A new form of flutter-margin has been developed for a trinary flutter, which also varies in a sensibly linear manner with dynamic pressure; it is also relatively insensitive to errors in damping, but is very sensitive to errors in frequency.

Nomenclature

A_{ij}	= constants in coefficients of characteristic equation
a_1-a_4	= quasisteady aerodynamic coefficients
B_0-B_2	= coefficients in flutter-margin expression
b	= airfoil semichord
b_1-b_4	= quasisteady aerodynamic coefficients
$C_{L\alpha}$	= lift curve slope
c	= airfoil chord
F	= flutter-margin
h	= nondimensional displacement of the airfoil in the plunging, or heave, direction
I	= moment of inertia per unit length
m	= airfoil mass per unit length
p_6-p_0	= coefficients in the characteristic equation
q	= dynamic pressure
T_i	= stability test determinants
T_{ijk}	= coefficients in expansions of test determinants
V	= velocity
α	= angular displacement of the airfoil in the pitch direction
β_i	= real part of eigenvalue i
ε	= $k_h x/ml$
ζ_α, ζ_h	= viscous damping coefficient for pitching and plunging motion
λ	= eigenvalue
ρ	= density of air
σ	= I/mc^2
ω_α, ω_h	= frequency of oscillation in the pitch and plunge directions
ω_i	= imaginary part of eigenvalue i

Introduction

AIRCRAFT flutter is often a catastrophic phenomenon, and thus, prediction of its onset is essential. The uncertainties in flutter calculations are such that the aircraft's integrity must be confirmed by means of flight testing. Traditionally, this is done by increasing q in flight in small steps; at each step the damping and frequency of the aircraft's aeroelastic modes are measured. A decision is then made regarding the anticipated structural stability of the aircraft at the next increment of q ; this decision possibly being based on the past "trend" of the modal damping.¹ Unfortunately, the nature of flutter is such that sometimes the modal aeroelastic damping will increase continually till just prior to instability, and then decrease suddenly—so-called explosive flutter. Furthermore, *a priori*, it is not known which mode will go unstable, therefore, a sufficient number of modes must be monitored; also, almost certainly, there will be some experimental scatter in the modal damping measurements.² Thus, there is considerable uncertainty concerning whether or not instability will occur at the next increment of q .

One method of reducing this uncertainty is the so-called "flutter-margin method,"³ which makes use of both the modal frequency and damping information. Zimmerman and Weissenburger³ show that the flutter-margin varies in a much more gradual manner with q than does the modal damping; in particular, there is a steady decrease in flutter-margin to zero as instability is approached. An investigation of the use of the flutter-margin method on wind-tunnel aeroelastic data is given by Bennett,⁴ and a description of its use for flight test data by Katz et al.⁵

Unfortunately, this method is applicable to binary instabilities only, and is restricted to cases where the aerodynamic center remains fixed (subsonic or supersonic flight). Furthermore, the effect of experimental error, in either the frequency or damping measurements, is not known.

In this article, examples of this method are given based on simulated experimental data; the complications associated with multiple modes are discussed, as are the uncertainties associated with errors in the damping and frequency measurements.

Review of the Flutter-Margin Method

The flutter-margin method³ is based on the analysis of a two degree-of-freedom (plunging and torsion) airfoil shown

Received Nov. 19, 1991; revision received March 23, 1992; accepted for publication March 25, 1992; presented as Paper 92-2101 at the AIAA Dynamics Specialist Conference, Dallas, TX, April 16–17, 1992. Copyright © 1991 by the American Institute of Aeronautics and Astronautics, Inc. All rights reserved.

*Associate Professor, Department of Mechanical Engineering, Member AIAA.

†Senior Research Officer, High Speed Aerodynamics Laboratory, National Research Council. Member AIAA.

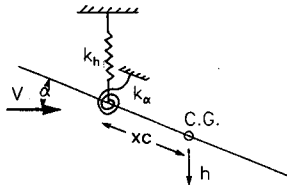


Fig. 1 Typical section with two DOF.

in Fig. 1. Using quasisteady aerodynamics it is easy to show that the airfoil is stable if F is greater than zero, where F is given by

$$F = [(p_2/2)^2 - p_0] - [(p_2/2) - p_1/p_3]^2 \quad (1)$$

and p_3 to p_0 are coefficients of the system's characteristic equation

$$\lambda^4 + p_3\lambda^3 + p_2\lambda^2 + p_1\lambda + p_0 = 0 \quad (2)$$

Furthermore, Zimmerman and Weissenburger³ show that for two modes with no structural damping and a fixed aerodynamic center, F can be written in the following form:

$$F = B_2(C_{L\alpha}q)^2 + B_1(C_{L\alpha}q) + B_0 \quad (3)$$

where B_2 , B_1 , and B_0 are only weakly dependent on q and may be taken as constants. The "heart" of the flutter-margin method is that F varies in a much more gradual manner with q than does the modal damping. Assuming that the modal damping and frequency have been measured at a particular velocity, then the "experimental eigenvalues" may be evaluated as follows:

$$\lambda_{1,2} = \beta_1 \pm i\omega_1$$

where, assuming the modal damping to be small, ω_1 is the frequency of mode 1, $\beta_1 = \delta_1\omega_1/(2\pi)$ and δ_1 is the logarithmic decrement of mode 1; similarly for $\lambda_{3,4}$. To evaluate F , the characteristic equation written as

$$(\lambda - \lambda_1)(\lambda - \lambda_2)(\lambda - \lambda_3)(\lambda - \lambda_4)$$

is equated with Eq. (2) to give

$$\begin{aligned} p_3 &= -2(\beta_1 + \beta_2) \\ p_2 &= \beta_1^2 + \beta_2^2 + \omega_1^2 + \omega_2^2 + 4\beta_1\beta_2 \\ p_1 &= -2[\beta_1(\beta_2^2 + \omega_2^2) + \beta_2(\beta_1^2 + \omega_1^2)] \\ p_0 &= (\beta_1^2 + \omega_1^2)(\beta_2^2 + \omega_2^2) \end{aligned} \quad (4)$$

The flutter-margin is then calculated using Eq. (1). Extrapolating from the known data points, using a quadratic in q , leads to the predicted dynamic pressure at which flutter occurs.

Extensions to the Two-Mode Flutter-Margin Method

For a two-mode system with no structural damping, quasisteady aerodynamics, and incompressible flow, F varies as a quadratic in q . However, if any of these restrictions are lifted, the variation of F with q is much more complicated. In this section the effect of more complex aerodynamics and structural damping are examined.

Considering the simple model shown in Fig. 1, and then as shown in the Appendix, using a general form of aerodynamics with " h " dependence allowed for, F for zero structural damping is given by Eq. (A4) and for the more general case, including the structural damping, by Eq. (A5). The inclusion of the h -dependent terms accounts for a more general form of unsteady aerodynamics; although one where the frequency

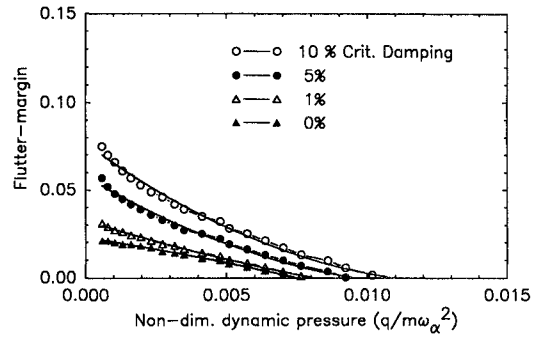


Fig. 2 Variation of the flutter-margin, obtained using Eq. (A5), with dynamic pressure and curves showing a quadratic fit to the data; $m/(\pi pb^2) = 100$, $\omega_h/\omega_\alpha = 0.2$, E.A. at $\frac{1}{4}c$, C.G. at $\frac{3}{8}c$ ($\epsilon = 0.005$), $I/(mc^2) = 0.0625$, $k = 0.2$.

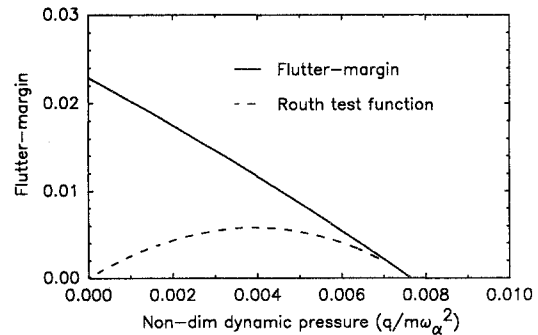


Fig. 3 Variation of the Routh stability test function and flutter-margin with dynamic pressure; $m/(\pi pb^2) = 100$, $\omega_h/\omega_\alpha = 0.2$, E.A. at $\frac{1}{4}c$, C.G. at $\frac{3}{8}c$ ($\epsilon = 0.005$), $I/(mc^2) = 0.0625$, $k = 0.2$, $\zeta_\alpha = \zeta_h = 0.0$.

is still held constant, a "p-type" analysis. With zero structural damping, F is indeed a quadratic in q , in agreement with Zimmerman and Weissenburger,³ although there does seem to be some disagreement in the constants of the quadratic. It is worthwhile pointing out that many checks have been done to ensure the correctness of the expressions given in the Appendix. Possibly, the most telling of these is that for typical values of system parameters, the flutter-margin was used to predict the flutter speed, this was then checked with a standard eigenvalue analysis.

For the more general case, where structural damping is included, F is given by a much more complex expression, Eq. (A5). Having obtained Eq. (A5), it is of interest to see how the predicted flutter-margin varies with q , this was done for the following parameters: $m/(\pi pb^2) = 100$, $\omega_h/\omega_\alpha = 0.2$, elastic axis (E.A.) at $\frac{1}{4}c$, c.g. at $\frac{3}{8}c$ ($\epsilon = 0.005$), $I/(mc^2) = 0.0625$ and $\zeta_\alpha = \zeta_h$ and varying from 0 to 10% of critical damping. The aerodynamic coefficients were taken as $a_1 = 5.375$, $a_2 = -10.63$, $a_3 = -1.975$, $a_4 = 4.572$, $b_1 = 2.750$, $b_2 = -8.458$, $b_3 = 1.239$, $b_4 = 2.286$, which were obtained using $k = 0.2$ in Theodorsen's function.⁶ The variation in F for four levels of structural damping is presented in Fig. 2 as a function of nondimensional dynamic pressure, $q/(m\omega_\alpha^2)$. Provided the data points at very low velocities are neglected, F is well-represented by a quadratic in q ; this was verified for many different sets of parameters.

Additional Forms of Flutter-Margin

For the characteristic equation given by Eq. (2), the flutter-margin is not a unique indicator of flutter. For example, the more conventional expression for the Routh stability test function for this characteristic equation is

$$F = p_1(p_3p_2 - p_1) - p_3^2p_0 \quad (5)$$

If the Routh stability test function is employed as a potential indicator of flutter then its variation with q is not nearly so well-behaved vis-à-vis the flutter margin, as shown in Fig. 3. The flutter-margin has a much better form for extrapolating to the flutter boundary than does the Routh stability test function, its approach to instability being much more gradual.

Flutter-Margin Method for Three Modes

In this section an attempt is made to obtain a simple analytical expression for a flutter-margin test function for a trinary flutter. An example of a trinary flutter is given by Collar and Simpson,⁷ where the equations of motion for a four degree-of-freedom system are given.

An eigenvalue solution to these equations showed that the mode with the highest frequency did not play an active role in the flutter. However, if the mode with the lowest frequency is also removed, leaving only two modes, then no flutter is obtained. This demonstrates that three modes (fundamental and first overtone wing bending and fundamental wing torsion) are required for flutter to occur. Thus, this would seem to be a good system to use to test an equivalent expression to that given by Zimmerman and Weissenburger for a trinary flutter.

First, the characteristic equation of the system is written as

$$p_6\lambda^6 + p_5\lambda^5 + p_4\lambda^4 + p_3\lambda^3 + p_2\lambda^2 + p_1\lambda + p_0 = 0 \quad (6)$$

with the coefficients p_6 to p_0 given by

$$\begin{aligned} p_6 &= A_{60}, \quad p_5 = A_{51}V \\ p_4 &= A_{42}V^2 + A_{40}, \quad p_3 = A_{33}V^3 + A_{31}V \\ p_2 &= A_{24}V^4 + A_{22}V^2 + A_{20} \\ p_1 &= A_{15}V^5 + A_{13}V^3 + A_{11}V \\ p_0 &= A_{06}V^6 + A_{04}V^4 + A_{02}V^2 + A_{00} \end{aligned}$$

and the terms A_{60} – A_{00} are constants, which for the sake of brevity are not given here.

Next, the Routh stability criteria is used to determine the stability boundary; this is done by forming the test determinants T_1 – T_5 , all of which must be positive for the system to be stable. These test determinants are of the form

$$\begin{aligned} T_1 &= T_{11}V, \quad T_2 = T_{23}V^3 + T_{21}V \\ T_3 &= T_{36}V^6 + T_{34}V^4 + T_{32}V^2 \\ T_4 &= T_{410}V^{10} + T_{48}V^8 + T_{46}V^6 + T_{44}V^4 + T_{42}V^2 \\ T_5 &= T_{515}V^{15} + T_{513}V^{13} + T_{511}V^{11} + T_{59}V^9 \\ &\quad + T_{57}V^7 + T_{55}V^5 + T_{53}V^3 \end{aligned} \quad (7)$$

where the constants T_{11} – T_{53} are independent of V . The dynamic stability boundary is given by $T_5 = 0$, and thus, only the T_5 test function needs to be monitored (T_5 is written in terms of T_1 – T_4 and so it is still necessary to evaluate these).

Obviously, it is necessary to confirm that the above expressions are correct. This was done by evaluating the test function variation with velocity using the above expressions and also from the eigenvalues of the matrix equations. The two methods gave identical results, confirming that the above expressions are indeed correct.

Unfortunately, as seen from Fig. 4 the variation of test function, T_5 (normalized with respect to its maximum value), with V^2 (equivalent to the variation with dynamic pressure at constant air density) is not particularly convenient for extrapolating from a subcritical velocity to the flutter boundary; the large "hump" in the curve proving troublesome. However, as shown previously, the form of the test function is not unique and other forms, of a more beneficial nature, can be

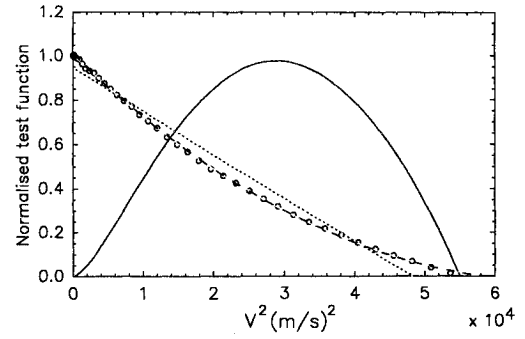


Fig. 4 Variation of the normalized test function T_5 and T_5/p_3^3 for a three degree-of-freedom system with velocity squared: —, T_5 ; ○, T_5/p_3^3 ; ---, quadratic fit to T_5/p_3^3 ; ·····, linear fit to T_5/p_3^3 .

established. Therefore, an attempt was made to obtain a new test function which varied in a more convenient manner. Several different possibilities were tried, and one of the "better" ones (T_5/p_3^3) is also shown in Fig. 4 (normalized such that its maximum value is of order 1); it should be stressed that all the test functions predict exactly the same flutter velocity. The new test function is of the form

$$\begin{aligned} F &= (T_{515}V^{12} + T_{513}V^{10} + T_{511}V^8 + T_{59}V^6 + T_{57}V^4 \\ &\quad + T_{55}V^2 + T_{53})/A_{51}^3 \end{aligned} \quad (8)$$

Unfortunately, there are seven constants in this expression which therefore make it impractical to use as a form to curve fit experimental data. Thus, an order of magnitude analysis was done to establish which, if any, of the terms in this expression can be neglected. The numerical values of the terms in the equation were evaluated for different velocities from zero to just past the point of instability. The V^{12} term is 3 orders of magnitude smaller than the others and can be neglected; for velocities almost up to the point of instability the V^{10} term is also small and can be neglected; the V^8 and V^6 terms are of approximately equal magnitude but of opposite sign, and thus, cancel each other out; this leaves the V^4 , V^2 , and V^0 terms. Thus, it is suggested that for curve fitting experimental data a test function of the form

$$F = AV^4 + BV^2 + C$$

be employed, where A , B , and C are constants and F is given by T_5/p_3^3 . As shown in Fig. 4, a quadratic in V^2 does give an excellent fit to the exact data points, also shown for comparison is a linear fit in V^2 which also gives a reasonable approximation to the data. The magnitude of the expression T_5/p_3^3 is usually very large, typically being of order 10^{19} . Such large numbers are cumbersome to deal with, and it is suggested that the expression be normalized by dividing all calculated values by the specific value at the lowest velocity for which the data is available; this will typically force the normalized T_5/p_3^3 to vary in the range 0 to 1; this was done for all the figures in this article.

To use the three-mode flutter-margin for flight test data, the procedure is a little more complicated than for a binary system, the characteristic equation may be written as

$$(\lambda - \lambda_1)(\lambda - \lambda_2)(\lambda - \lambda_3)(\lambda - \lambda_4)(\lambda - \lambda_5)(\lambda - \lambda_6)$$

which when equated with Eq. (6) gives

$$\begin{aligned} p_6 &= 1 \\ p_5 &= -2(\beta_1 + \beta_2 + \beta_3) \\ p_4 &= \beta_1^2 + \beta_2^2 + \beta_3^2 + \omega_1^2 + \omega_2^2 + \omega_3^2 \\ &\quad + 4(\beta_1\beta_2 + \beta_1\beta_3 + \beta_2\beta_3) \end{aligned}$$

$$\begin{aligned}
p_3 &= -2\beta_1(\beta_2^2 + \omega_2^2 + \beta_3^2 + \omega_3^2) \\
&\quad - 2\beta_2(\beta_1^2 + \omega_1^2 + \beta_3^2 + \omega_3^2) \\
&\quad - 2\beta_3(\beta_1^2 + \omega_1^2 + \beta_2^2 + \omega_2^2) + 8\beta_1\beta_2\beta_3 \\
p_2 &= (\beta_1^2 + \omega_1^2)(\beta_2^2 + \omega_2^2) + (\beta_1^2 + \omega_1^2)(\beta_3^2 + \omega_3^2) \\
&\quad + (\beta_2^2 + \omega_2^2)(\beta_3^2 + \omega_3^2) + 4\beta_1\beta_2(\beta_3^2 + \omega_3^2) \\
&\quad + 4\beta_1\beta_3(\beta_2^2 + \omega_2^2) + 4\beta_2\beta_3(\beta_1^2 + \omega_1^2) \\
p_1 &= -2\beta_3(\beta_1^2 + \omega_1^2)(\beta_2^2 + \omega_2^2) \\
&\quad - 2\beta_2(\beta_1^2 + \omega_1^2)(\beta_3^2 + \omega_3^2) \\
&\quad - 2\beta_1(\beta_2^2 + \omega_2^2)(\beta_3^2 + \omega_3^2) \\
p_0 &= (\beta_1^2 + \omega_1^2)(\beta_2^2 + \omega_2^2)(\beta_3^2 + \omega_3^2)
\end{aligned}$$

Given the frequency and damping, numerical values of the coefficients p_0 – p_5 are calculated and then substituted into the expression T_s/p_3^2 giving the new flutter-margin.

An attempt at obtaining a flutter-margin for flutter mechanisms involving more than two modes was also presented by Kadrnka.⁸ He investigated the stability of a system with multiple modes using two methods: 1) the Routh stability criteria (exactly the same as presented here), and 2) Mikhailov's stability criteria as discussed by Popov.⁹ Kadrnka showed that the two approaches produce exactly the same expression for the stability criteria. The disadvantage of the method proposed by Kadrnka, however, is that his flutter-margin is purely the determinant of the appropriate Routh test determinant; e.g., T_s . As shown previously, the variation of T_s with V is not convenient for extrapolating to the flutter speed. This is exactly the same sort of variation obtained by Kadrnka. He attempted to overcome this problem by curve fitting the flutter-margin variation with much higher polynomials than those used here, e.g., polynomials of order 4 or 6. This, however, is not likely to be possible when using real flight test data, especially when errors in the frequency and damping measurements are considered.

Use of $qC_{L\alpha}$, q or V

For a binary flutter with no structural damping, Zimmerman and Weissenburger³ obtained Eq. (3) which enables the effects of compressibility to be incorporated by way of the $C_{L\alpha}$ term—provided the variation of $C_{L\alpha}$ with Mach number is known. However, to do this it was necessary to assume that all the aerodynamic coefficients varied with Mach number in the same manner as $C_{L\alpha}$.

A reduced form of the above flutter-margin, with no variation in Mach number and no structural damping (see the Appendix), is of the form

$$F = Aq^2 + Bq + C$$

where A , B , and C are now totally independent of q . However, when the effect of either structural damping in a binary flutter or a trinary flutter is considered, then the algebra is such that the flutter-margin can only be reduced to

$$F = AV^4 + BV^2 + C$$

This suggests that the flutter-margin method can be used for flight testing at a constant air density (or altitude) only. However, as shown in Fig. 5, changes in air density have a relatively small effect on the variation of F with q , and in many cases can probably be ignored. In Fig. 5a the variation of F is presented for the same example as that used in Fig. 2 for 5% critical damping and two extremely different values of air density; slightly different flutter-margin variations are obtained. However, this is a very large variation in air density, and also a fairly large value of structural damping. With less

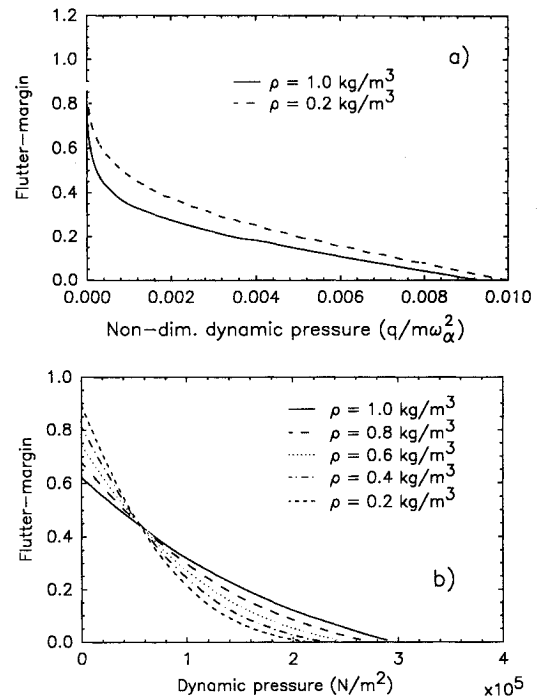


Fig. 5 Variation of flutter-margin with dynamic pressure for different air densities: a) a binary flutter, $m/(\pi pb^2) = 100$, $\omega_h/\omega_\alpha = 0.2$, $\varepsilon = 0.005$, $\sigma = 0.0625$, $\zeta_\alpha = \zeta_h = 0.05$; b) a trinary flutter from Collar and Simpson.⁷

structural damping and for smaller changes in air density these two curves could sensibly be collapsed onto one with little loss of accuracy.

For the trinary flutter example of Fig. 4, the effect of varying the air density is shown in Fig. 5b (this was obtained by assuming the original equations correspond to an air density of 1.0 kg/m^3). Again the flutter-margin variations do not collapse onto one curve, but for a reasonably small variation in air density, plotting F as a function of q will introduce a relatively small error.

Critical Assessment of the Flutter-Margin Method

To access the effectiveness of the flutter-margin method to predict the onset of flutter, a data-set given by Irwin and Guyett¹⁰ was employed. They present the variation of modal damping and frequency with velocity for six modes (the first four bending modes and first two torsional modes) of a swept-wing wind-tunnel model in subsonic flow; the data for the first three modes are replotted in Fig. 6. It is these three modes which have the most active variation as V is changed; for the other three modes there was little or no change in frequency with V and only a small and gradual increase in damping as V was increased. The most significant features of the modes shown in Fig. 6 are that it is mode 2 (the first overtone bending) which goes unstable at $V \approx 51.8 \text{ m/s}$ and that instability occurs very close to a frequency coalescence of modes 2 and 3 (fundamental torsion). It should also be noted that there is a fairly dramatic drop in the damping of mode 2 just prior to instability. One other interesting feature, which may possibly make this data-set atypical, is that at the flutter boundary, mode 1 is close to a divergence instability.

Two-Mode Combinations

Using the data of modes 2 and 3 from Fig. 6 the variation in F is as presented in Fig. 7, showing approximately a linear variation with V^2 . Using both parabolic and linear extrapolations of F with V^2 , predictions of the flutter speed are made at a number of velocities using all the previous data points. The results obtained are summarized in Table 1; quite reasonable predictions of the flutter speed can be made for ve-

locities down to 50% of the actual flutter speed. However, F seems to be sensibly linear in V^2 ; thus, the flutter speed is also predicted using a linear extrapolation in V^2 . Although the linear extrapolation is a little less accurate at higher speeds, it is much more accurate than the quadratic extrapolation at lower speeds, and thus, seems to be preferable.

If the two coalescing modes are not used to form the flutter margin then the variation of F with V^2 is no longer useful to predict the flutter speed. For example, if modes 1 and 2 are employed, F is essentially constant over the majority of the V^2 range, and then drops very sharply to zero at the point of

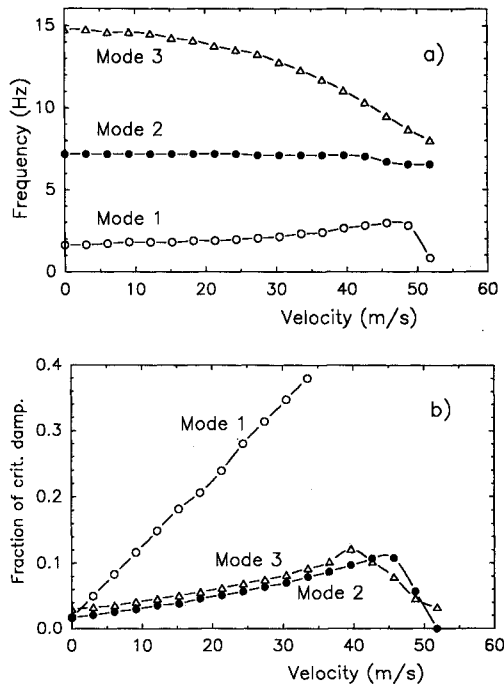


Fig. 6 Variation of aeroelastic modal frequencies and damping values with velocity for the first three of the six modes from Irwin and Guyett¹⁰: mode 1 is the fundamental bending, mode 2 the second harmonic bending, and mode 3 the fundamental torsion: a) frequencies and b) damping.

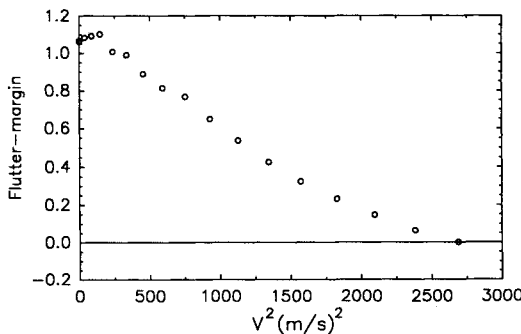


Fig. 7 Variation of the flutter-margin with velocity squared obtained using the Zimmerman and Weissenburger³ method and the data of modes 2 and 3 from Irwin and Guyett.¹⁰

instability. If modes 1 and 3 are employed, F will always remain positive—it is mode 2 which becomes unstable.

In addition to the above data-set, a hypothetical data-set was made up to simulate the case of a single degree-of-freedom flutter. This could, for example, be representative of a stall flutter. The model represented by Fig. 1 was analyzed with $m/(\pi pb^2) = 100$, $\varepsilon = 0.0$, $\sigma = 0.0625$ and $\zeta_h = \zeta_a = 0.05$; however, the aerodynamic coefficients were arbitrarily changed to $a_1 = a_2 = b_3 = b_4 = 0.0$, $a_3 = 1.975$, $a_4 = 4.572$, $b_1 = -2.75$, and $b_2 = 2.45$ (these were chosen to give a single degree-of-freedom flutter). An eigenvalue analysis showed that there is no frequency coalescence and instability is purely due to negative damping in the torsional direction (indeed, it should be noted that there is no coupling, either structural or aerodynamic, between the equations for this set of parameters). The variation in F with nondimensional dynamic pressure for two examples is presented in Fig. 8. It is apparent that for $\omega_h/\omega_a = 0.8$ the variation in F is similar to that obtained with a classical frequency coalescence; however, for $\omega_h/\omega_a = 0.2$ the variation in F is not so nearly well behaved. Undoubtedly, the reason for this is that the initial separation of the two frequencies, which is maintained all the way until the onset of flutter “tricks” the flutter-margin into believing that an instability is not going to occur. Only at the last minute, when the damping is very close to zero, does the damping start to dominate the flutter-margin calculations and causes it to go to zero. Thus, it is apparent that the flutter-margin method is not very useful at predicting the onset of flutter for single degree-of-freedom-type instabilities.

Damping and Frequency Errors for Two-Mode Combination

Having established that good predictions of the flutter speed can be obtained when accurate subcritical data is employed, it now remains to be seen what is the effect of errors in the damping and frequency measurements. To this end, simulated errors were added to the data of Irwin and Guyett.¹⁰ A maximum allowable error in frequency and damping was decided upon, and then for each data point an error term equal to this maximum multiplied by a random number between ± 1 was added to the original data point. In general, the maximum allowable error for the damping measurements was greater than for the frequency measurements, this is usually the case for experimental flight test data.²

The effect of errors in the damping and frequency measurements was also investigated by Bennett⁴ and Kadrnka,⁸

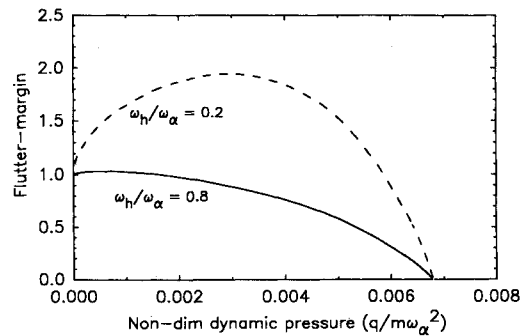


Fig. 8 Variation of the flutter-margin with dynamic pressure: $m/(\pi pb^2) = 100$, $\varepsilon = 0.0$, $\sigma = 0.0625$, $a_1 = a_2 = b_3 = b_4 = 0.0$, $a_3 = 1.975$, $a_4 = 4.572$, $b_1 = -2.75$, $b_2 = 2.45$.

Table 1 Comparison of predicted flutter speed using the flutter-margin for data taken from Irwin and Guyett¹⁰—the true flutter speed is 51.8 m/s

A, m/s	48.8	45.7	42.7	39.6	36.6	33.5	30.5	27.4	24.4	21.3	18.3
B, m/s	50.0	48.5	46.9	45.4	44.2	43.0	41.8	41.1	35.1	31.4	29.0
C, m/s	48.5	47.6	46.9	46.6	46.6	46.9	47.6	48.5	48.2	50.6	59.7

A) Speed at which prediction is made (using all previous data).

B) Flutter speed obtained using a quadratic extrapolation in V^2 .

C) Flutter speed obtained using a linear extrapolation in V^2 .

who calculated the partial derivatives of F with respect to the modal damping and frequencies.

For a maximum allowable error of 10% in damping and 5% in frequency, the variation in F with V^2 is shown in Fig. 9a. Comparing this with Fig. 7, it is apparent that the effect of the error is to produce a fairly large scatter in F . Calculations of this type were done for a number of different allowable maximum errors and one immediate conclusion is that F is much more sensitive to errors in frequency than in damping. For example, Fig. 9b shows the variation of F for the case where the frequency error has been reduced to zero but the damping error is still 10%; comparing this with Fig. 7 shows that the error in damping has produced very little deterioration in the variation in F .

A summary of the effect of the errors is presented in Table 2. In general, as the error increases, particularly an error in frequency, the accuracy of the estimated flutter speed decreases. It is also interesting to note that the errors have less

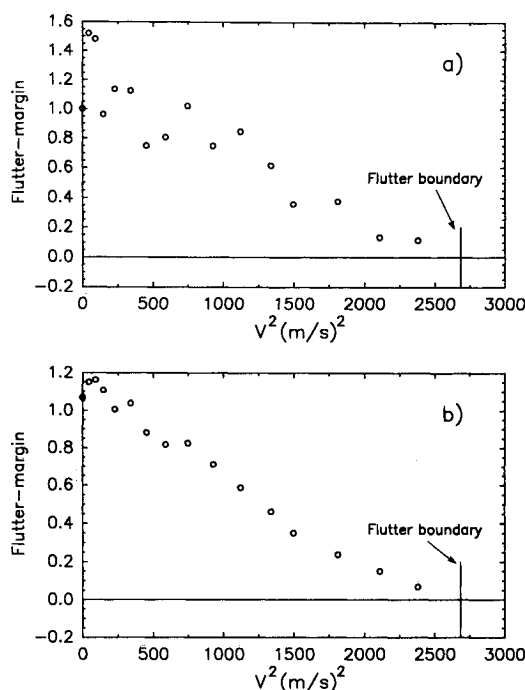


Fig. 9 Effect of errors in the damping and frequency on the variation of the flutter-margin; modes 2 and 3 of Irwin and Guyett¹⁰: a) a maximum 5% error in frequency and 10% error in damping, and b) a maximum 0% error in frequency and 10% error in damping.

Table 2 Effect of errors in damping and frequency measurements on the predicted flutter speed (m/s) using data for modes 2 and 3 of Irwin and Guyett¹⁰—true flutter speed is 51.8 m/s

Error		A	B	C	D
Freq, %	Damp, %				
5	10	48.5	48.8	43.9	49.7
3	10	46.6	48.5	39.9	49.7
5	7	48.5	48.8	43.3	49.7
5	0	48.5	48.8	44.2	49.4
7	10	∞	45.4	47.2	42.7
7	0	∞	45.4	∞	42.7
0	15	48.2	47.9	∞	42.7
10	0	46.6	48.5	38.4	50.0

A) Flutter speed predicted from an actual speed of 45.7 m/s using a quadratic extrapolation in V^2 .

B) Flutter speed predicted from an actual speed of 45.7 m/s using a linear extrapolation in V^2 .

C) Flutter speed predicted from an actual speed of 36.6 m/s using a quadratic extrapolation in V^2 .

D) Flutter speed predicted from an actual speed of 36.6 m/s using a linear extrapolation in V^2 .

effect on the linear extrapolation than on the quadratic one. This seems to suggest that for real flight data, which will undoubtedly have significant errors, a linear extrapolation is a better prediction tool than a quadratic one for the onset of flutter.

Three-Mode Combination

As seen in Fig. 4, if the new flutter-margin (T_s/p_s^3) is employed there is a reasonably linear variation in F with V^2 , at least for the data coming from the calculations of Collar and Simpson.⁷ What is surprising about this data-set is that if a quadratic curve fit is employed to extrapolate to the flutter speed from a subcritical speed, then flutter is never predicted. This can be seen in Fig. 10, where a quadratic curve is fitted to all the data below 192 m/s (0.81 of the flutter speed). The curve fits the data almost exactly—showing that a quadratic curve is a good curve fit—but then curls up just past the last point; thus, based on this quadratic curve fit, flutter is never predicted. This demonstrates one of the dangers of extrapolation and particularly of using a quadratic extrapolation of the flutter-margin to predict flutter. If a linear fit is employed, on the other hand, then a reasonable curve fit is obtained as also shown in Fig. 10. Also, if the data points for the lower velocities are ignored (these would, in fact, not be available from flight test data) then an even better curve fit is obtained and good predictions of the flutter speed can be obtained from speeds as low as 30% of the flutter speed; this is illustrated in Table 3.

Although this was the only true trinary flutter known to the authors, it was decided to see if this new flutter-margin could give accurate predictions of flutter for a binary flutter when a third noncoalescing mode is included. To achieve this the data-set of Irwin and Guyett¹⁰ was employed with all three active modes now included. The resulting variation in the new flutter-margin (T_s/p_s^3) with V^2 is presented in Fig. 11, again the data points at low velocities have been ignored. It is apparent that a reasonable prediction of the flutter speed could be obtained with a linear extrapolation; this prediction getting better as the flutter velocity is approached; however, in general, it is suggested that not only should the trinary flutter-margin be monitored, but also the various combinations of binary flutter-margins, to detect any effect from a passive mode.

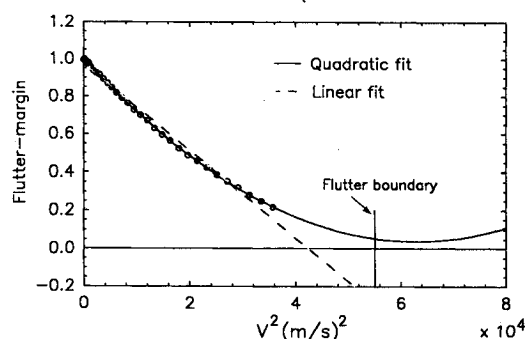


Fig. 10 Variation of new test function, T_s/p_s^3 , with velocity squared: data from Collar and Simpson⁷; —, a quadratic fit to this test function for all data points below a velocity of 192.0 m/s; ---, a linear fit to this test function for all data points with velocities between 137.2 and 192.0 m/s.

Table 3 Linear extrapolation in velocity squared using all data above a velocity of 137.2 m/s for the new flutter-margin (T_s/p_s^3)—the true flutter speed is 237.7 m/s

A, m/s	231.6	213.4	189.0	164.6	140.2	109.7	85.3	61.0	36.6
B, m/s	219.5	213.4	206.0	199.3	193.5	189.3	186.8	185.6	188.1

Variation of predicted flutter speed (row B) with actual speed at which the prediction is made (row A) for the trinary flutter of Collar and Simpson.⁷

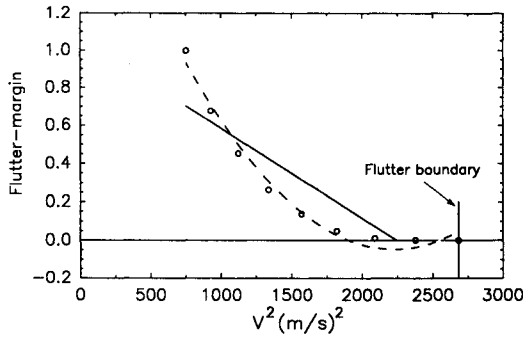


Fig. 11 Variation of new test function, T_s/p_s^3 , with velocity squared using all three active modes from Irwin and Guyett¹⁰ and linear and quadratic curve fits for data points with velocities greater than 33.5 m/s.

Table 4 Linear extrapolation in velocity squared for the new flutter-margin (T_s/p_s^3)—the true flutter speed is 237.7 m/s

A, m/s	231.6	219.5	207.3	195.1	182.9	170.7	158.5	134.1	109.7
B, m/s	235.6	210.0	205.1	200.6	196.9	188.4	182.3	192.9	313.9

Variation of predicted flutter speed (row B) with actual speed at which the prediction is made (row A) for the trinary flutter of Collar and Simpson⁷ with a simulated error of 5% in frequency and 10% in damping.

Damping and Frequency Errors for Three-Mode Combination

The effect of simulated errors in frequency and damping on the new flutter-margin was investigated for the trinary flutter using the same method as that described for the two-mode combination. The nature of the results obtained was very similar to that obtained with a binary flutter; the flutter-margin being much more sensitive to errors in frequency than in damping. However, using a linear extrapolation in F with V^2 it is still possible to obtain reasonable predictions of the flutter speed as shown in Table 4.

Conclusions

Based on the results presented in this article the following conclusions can be obtained; however, it should be appreciated that these conclusions may be specific to the examples analyzed in this article.

1) Using the two active modes in a binary flutter, it is shown that when no structural damping is accounted for and the aerodynamics is taken as being quasisteady, the flutter-margin is exactly a quadratic function of dynamic pressure. However, it is also apparent that the flutter-margin varies in a sensibly linear manner with dynamic pressure; this is so, irrespective of whether or not structural damping is accounted for.

2) Using either a linear or quadratic extrapolation in dynamic pressure, it is possible to predict the onset of flutter from velocities as low as 50% of the flutter speed.

3) The flutter-margin variation is very sensitive to errors in the modal frequencies and only mildly sensitive to errors in the modal damping. When errors in the frequency and damping measurements are accounted for it appears that a linear extrapolation is the best method of predicting the onset of flutter.

4) The flutter-margin method does not vary in a well-behaved manner with dynamic pressure when the instability mechanism is dominated by a single degree of freedom (DOF). In such cases the flutter-margin method would not be able to accurately predict the flutter speed.

5) For a trinary flutter, a new form of the flutter-margin is suggested which is of the form T_s/p_s^3 . This new form of flutter-margin also varies in a sensibly linear manner with dynamic pressure. The effect of errors in the damping and frequency measurements on the trinary flutter-margin variation is very similar to that obtained with the binary flutter-margin.

Appendix: Extension of the Zimmerman and Weissenburger Method

Considering the model shown in Fig. 1, the equations of motion about the center of gravity may be written as

$$\begin{aligned} \ddot{h} + 2\zeta_h\omega_h\dot{h} + \omega_h^2h - \varepsilon\alpha &= (q/m)[a_1\alpha + a_2(c/V)\dot{\alpha} \\ &+ a_3h + a_4(c/V)\dot{h}] \\ \sigma\ddot{\alpha} + 2\sigma\zeta_\alpha\omega_\alpha\dot{\alpha} + \sigma\omega_\alpha^2\alpha - \varepsilon\sigma h &= (q/m)[b_1\alpha + b_2(c/V)\dot{\alpha} \\ &+ b_3h + b_4(c/V)\dot{h}] \end{aligned} \quad (A1)$$

where

$$\begin{aligned} \omega_h^2 &= k_h/ml, \quad \omega_\alpha^2 = (k_\alpha + k_h x^2 c^2)/Il \\ \varepsilon &= k_h x/ml, \quad \sigma = Ilmc^2 \end{aligned}$$

and ζ_h and ζ_α are the nondimensional damping coefficients.

The eigenvalues of the above equations satisfy the following characteristic equation:

$$\lambda^4 + p_3\lambda^3 + p_2\lambda^2 + p_1\lambda + p_0 = 0$$

where

$$\begin{aligned} p_3 &= A_{31} + UA_{32} \\ p_2 &= A_{21} + q_b A_{22} + UA_{23} \\ p_1 &= A_{11} + q_b A_{12} + q_b UA_{13} + UA_{14} \\ p_0 &= A_{01} + q_b A_{02} + q_b^2 A_{03} \\ q_b &= q/m \\ U &= qc/mV \end{aligned} \quad (A2)$$

The " A_{ij} " terms are all independent of velocity and are given by the following expressions:

$$\begin{aligned} A_{31} &= 2(\omega_\alpha\zeta_\alpha + \omega_h\zeta_h), \quad A_{32} = (\sigma a_4 - b_2)/\sigma \\ A_{21} &= \omega_\alpha^2 + \omega_h^2 + 4\omega_\alpha\omega_h\zeta_h\zeta_\alpha \\ A_{22} &= [\sigma a_3 - b_1 + \mu(a_2b_4 - b_2a_4)]/\sigma \\ A_{23} &= 2(a_4\sigma\omega_\alpha\zeta_\alpha - b_2\zeta_h\omega_h)/\sigma \\ A_{11} &= 2\omega_\alpha\omega_h(\omega_\alpha\zeta_h + \omega_h\zeta_\alpha) \\ A_{12} &= 2(-b_1\zeta_h\omega_h + \zeta_\alpha\omega_\alpha\sigma a_3)/\sigma \\ A_{13} &= (-b_1a_4 - b_2a_3 + a_2b_3 + a_1b_4)/\sigma \\ A_{14} &= [a_4\sigma\omega_\alpha^2 - b_2\omega_h^2 + \varepsilon(a_2 - b_4)]/\sigma \\ A_{01} &= (\sigma\omega_\alpha^2\omega_h^2 - \varepsilon^2)/\sigma \\ A_{02} &= (a_3\sigma\omega_\alpha^2 - b_1\omega_h^2 + a_1\varepsilon - b_3\varepsilon)/\sigma \\ A_{03} &= (-a_3b_1 + a_1b_3)/\sigma \\ \mu &= \frac{1}{2}\rho c^2/m \end{aligned} \quad (A3)$$

Making use of Eqs. (A3) and (A2), F may be evaluated. For the case of zero structural damping Eqs. (A3) are simplified somewhat, since

$$A_{31} = A_{23} = A_{11} = A_{12} = 0, \quad A_{21} = \omega_\alpha^2 + \omega_h^2$$

and all other terms remain unchanged. In this case the flutter-margin may be written as

$$F = D_0q_b^2 + D_1q_b + D_2 \quad (A4)$$

where

$$D_0 = [-A_{03} + A_{22}A_{13}/A_{23} - (A_{13}/A_{32})^2]$$

$$D_1 = [-A_{02} + A_{22}A_{14}/A_{32} + A_{21}A_{13}/A_{32} - 2A_{13}A_{14}/(A_{32})^2]$$

$$D_2 = [-A_{01} + A_{21}A_{14}/A_{32} - (A_{14}/A_{32})^2]$$

For the more general case where damping is included, the algebra is much more complicated. One problem is the $p_3 = A_{31} + UA_{32}$ term which appears in the denominator. However, bearing in mind that the A_{31} term is proportional to ζ and A_{32} is inversely proportional to σ , then $A_{32} \gg A_{31}$ and thus, $p_3 \approx UA_{32}$.

Making this assumption, F may be written as

$$F = q_b^2 C_0 + q_b U(C_5/\mu + C_6) + q_b(C_1 + C_{10}/\mu) + U(C_7 + C_4/\mu) + (C_2 + C_9/\mu) + 1/U(C_3) + 1/q_b(C_8/\mu) \quad (A5)$$

where C_0 – C_8 are independent of q_b ; they are functions of the "A" terms in Eq. (A3) and for the sake of brevity are not given.

Acknowledgments

The authors gratefully acknowledge the financial support of the Institute for Aerospace Research and the Canadian

Department of National Defence. S. J. Price also acknowledges the support of the Natural Sciences and Engineering Research Council of Canada and Le Fonds FCAR of Quebec.

References

- ¹Kordes, E. E., *Flutter Testing Techniques*, NASA SP-415, Oct. 1975.
- ²Koenig, K., "Problems of System Identification in Flight Vibration Testing," AGARD Rept. 720, Vimeriro, Portugal, Oct. 1983.
- ³Zimmerman, N. H., and Weissenburger, J. T., "Prediction of Flutter Onset Speed Based on Flight Testing at Subcritical Speeds," *Journal of Aircraft*, Vol. 1, No. 4, 1964, pp. 190–202.
- ⁴Bennett, R. M., "Application of Zimmerman Flutter-Margin Criterion to a Wind-Tunnel Model," NASA TM 84545, Nov. 1982.
- ⁵Katz, H., Foppe, F. G., and Grossman, D. T., "F-15 Flight Flutter Test Program," *Flutter Testing Techniques*, NASA SP-415, 1975, pp. 413–431.
- ⁶Theodorsen, T., "General Theory of Aerodynamic Instability and the Mechanism of Flutter," NACA Rept. 685, 1935.
- ⁷Collar, A. R., and Simpson, A., *Matrices and Engineering Dynamics*, Ellis Horwood Ltd., London, 1987.
- ⁸Kadrnka, E. E., "Multimode Instability Prediction Method," AIAA 26th Structures, Structural Dynamics and Materials Conf., AIAA Paper 85-0737-CP, Orlando, FL, April 1985.
- ⁹Popov, E. P., *The Dynamics of Automatic Control*, Pergamon, Oxford, England, UK, 1962.
- ¹⁰Irwin, C. A. K., and Guyett, P. R., "The Subcritical Response and Flutter of a Swept-Wing Model," *RAE Reports and Memoranda*, 3497, Farnborough, England, UK, Aug. 1965.

Recommended Reading from the AIAA Education Series

Introduction to Mathematical Methods in Defense Analyses

J.S. Przemieniecki

Reflecting and amplifying the many diverse tools used in analysis of military systems and as introduced to newcomers in the armed services as well as defense researchers, this text develops mathematical methods from first principles and takes them through to application, with emphasis on engineering applicability and real-world depictions in modeling and simulation. Topics include: Scientific Methods in Military Operations; Characteristic Properties of

Weapons; Passive Targets; Deterministic Combat Models; Probabilistic Combat Models; Strategic Defense; Tactical Engagements of Heterogeneous Forces; Reliability of Operations and Systems; Target Detection; Modeling; Probability; plus numerous appendices, more than 100 references, 150 tables and figures, and 775 equations. 1990, 300 pp, illus, Hardback, ISBN 0-930403-71-1, AIAA Members \$47.95, Nonmembers \$61.95, Order #: 71-1 (830)

Defense Analysis Software

J. S. Przemieniecki

Developed for use with *Introduction to Mathematical Methods in Defense Analyses*, *Defense Analysis Software* is a compilation of 76 subroutines for desktop computer calculation of numerical values or tables from within the text. The subroutines can be linked to generate extensive programs. Many subroutines can

also be used in other applications. Each subroutine fully references the corresponding equation from the text. Written in BASIC; fully tested; 100 KB needed for the 76 files. 1991, 131 pp workbook, 3.5" and 5.25" disks, ISBN 0-930403-91-6, \$29.95, Order #: 91-6 (830)

Place your order today! Call 1-800/682-AIAA



American Institute of Aeronautics and Astronautics
Publications Customer Service, 9 Jay Gould Ct., P.O. Box 753, Waldorf, MD 20604
Phone 301/645-5643, Dept. 415, FAX 301/843-0159

Sales Tax: CA residents, 8.25%; DC, 6%. For shipping and handling add \$4.75 for 1-4 books (call for rates for higher quantities). Orders under \$50.00 must be prepaid. Please allow 4 weeks for delivery. Prices are subject to change without notice. Returns will be accepted within 15 days.